PHASE NOISE COMPENSATION IN OPTICAL FIBER

Y. Baron[a], **M. Comba**[b]

a. Mines Paris – PSL + yannis.baron@etu.minesparis.psl.eu

b. Mines Paris – PSL + matti.comba@etu.minesparis.psl.eu

Key words : phase noise ; single mode optical fiber ; frequency modulation ; Michelson interferometer

Abstract :
Phase noise in single mode optical fiber can lead to to a deterioration of laser signals. The goal of this intership was to evaluate the phase noise generated in the fiber by the laboratory building to determine wether to implement a compensation system or not.

1 Introduction

To achieve satisfactory results in high resolution spectroscopy, lasers with high frequency stability and accuracy are required. Several laboratories are therefore specialized in the production of such hyper-precise lasers such as the SYRTE[1] which produces a highly stable infrared signal at 1542 nm with a relative stability better than 10^{-14} at any time scale. Such signals are then disseminated through optical fiber networks (REFIMEVE [2]) to other laboratories to be used as frequency references for other laser beams. However, the transfer through the optical fiber betweeen laboratories can induce phase noise in the signal caused by the variation of optical path induced by changes in outer temperature, pressure or other vibrations which thus deteriorate the stability of incoming signal.

Systems to cancel out this noise are already well-known and are extensively used by REFIMEVE. In the case of the LKB spectroscopy team, the REFIMEVE signal is used as reference for a frequency comb used in a trapped ions experiment. The REFIMEVE signal is being corrected between the SYRTE laboratory and the REFIMEVE extraction station at LKB. However, between the location of said signal and the experiment using the frequency comb, there are about 200 m of uncorrected optical fiber which could induce aforementioned phase noise. The goal of the study was to evaluate the phase noise induced in the laboratory's building in order to decide wether or not it would be useful to implement another noise cancellation system for these 200 m of fiber.

In order to carry out the evaluation, the system implemented is paradoxically the same as the one that cancels the noise The protocol used was mostly inspired of the one proposed by Long-Sheng Ma, Peter Jungner, Jun Ye and John L. Hall [**?**] and relies on a Michelson interferometer to measure phase noise.

In section 2, the system set up is introduced with the various tools used. Section 3 then delves into the results of the experiment and the interpretation of the results. Section 4 ends concludes this paper and reviews needed improvements for the system.

2 Tools

2.1 Equipments

To measure and compensate the phase noise, the following equipments are used.

[1] SYstèmes de Référence Temps-Espace, Observatoire de Paris – PSL / CNRS (UMR 8630)
[2] REseau FIbré MEtrologique à Vocation Européenne

2.1.1 Laser

A fiber laser of wavelength $\lambda = 1542$ nm is used in order to work close to the wavelength of the REFIMEVE signal. The model used is an NKT Photonics Koheras Basik which is tunable from 500 to 2100 nm and delivers up to 27 dBm (500 mW).

2.1.2 Faraday mirror

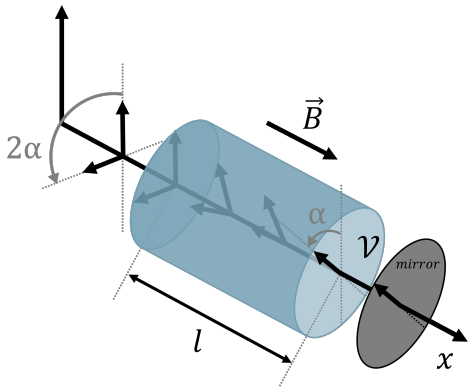

Figure 1: *A schematic Faraday mirror. The angle between the incident and the transmitted polarization is* 2α.

A Faraday mirror is the combination of a Faraday rotator and a mirror. As its name suggests, the mirror simply reflects the signal. The Faraday rotator uses the Faraday effect, which enables optically inactive mediums *(here terbium-gallium garnet)* to acquire different reflexive index, depending on the polarization of the signal when a static $\vec{B}$ field is applied to them.

This induces a rotation of the polarization for linearly polarized signals. This rotation is proportional to B in the propagation direction of the signal. This relation can be expressed as

$$\alpha = \mathcal{V} \cdot l \cdot B, \tag{1}$$

where l is the propagation length, and $\mathcal{V}$ is the Verdet constant (in $\mathrm{rad} \cdot \mathrm{T}^{-1} \cdot \mathrm{m}^{-1}$) [**?**].

The Faraday mirrors used in this paper induce a 45° rotation of the polarization of the incoming signal in both directions, resulting in the reflected polarization being orthogonal to the input polarization state *(considering the input polarization state to be linear)*. Thanks to this specific type of mirror, the polarization state of both arms match on the photodetector.

2.1.3 Acousto-optic modulator (AOM)

An acouto-optic modulator (AOM) allows to shift the frequency and phase of an optical signal using sound waves.

Using the piezoelectric effect, the AOM-powering electric signal drives a ceramic transducer to vibrate. This transducer creates sound waves in a quartz it is attached to. The succession of expansion and compression modulates the reflexive index $n(x,t) = n_0 + n_1 \cos(\Omega t - k_{AOM} x)$ where $\Omega = 2\pi f_{AOM}$, $k_{AOM} = \dfrac{2\pi f_{AOM}}{v}$ and v is the speed of sound in quartz.

The sound waves operate as a diffraction grating. Thus, the conservation of energy and momentum implies that the diffraction angles $\theta_{p\in\mathbb{Z}}$ for an incident angle θ_i are submitted to the following equations

$$\forall p \in \mathbb{Z} : \quad \sin\theta_p = \sin\theta_i + p \cdot \frac{\lambda_i}{\lambda_{AOM}} \tag{2}$$

$$\cos\theta_p = \cos\theta_i \tag{3}$$

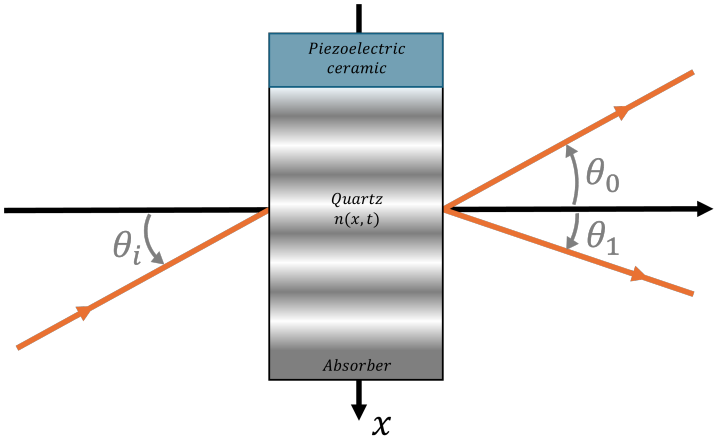

Figure 2: *A schematic AOM. The incident angle is θ_i. The diffraction order 1 angle is θ_1.*

where $\lambda_i = \lambda$ is the wavelength of the optical signal and λ_{AOM} is the wavelength of the AOM-powering signal.

When the incident beam arrives at Bragg's angle, the diffracted angles follow the equation [**?**]

$$\forall p \in \mathbb{Z} : \quad \sin\theta_p = p \cdot \frac{\lambda_i}{2\lambda_{AOM}} \tag{4}$$

For this paper, a fiber-coupled AOM is used, working at $f_{AOM} = 80$ MHz. The diffraction order 1 is coupled to the output fiber so that

$$\omega_p = \omega_i + \Omega \tag{5}$$
$$f_p = f_i + f_{AOM} \tag{6}$$

where ω_p (resp. f_p) is the angular frequency (resp. frequency) of the p-th diffracted beam, and ω_i (resp. f_i) is that of the incident beam. The optimal amplitude for the AOM-powering voltage was experimentally determined to be 90 mVpp by plotting the output power for different voltage amplitudes, as seen in figure 3. The acceptance at half maximum is ±2 MHz.

2.2 Photodiode and beatnote

A photodiode is a semi-conductor diode which produces an electric signal when absorbing photons. It can be used to determine the beatnote of two optical signals $\overrightarrow{E_1}$ and $\overrightarrow{E_2}$,

$$\overrightarrow{E_1} = E_1^0 \overrightarrow{\varepsilon_1} e^{i(\omega_1 t - \overrightarrow{k_1}\cdot\overrightarrow{r} + \varphi_1)} \qquad \overrightarrow{E_2} = E_2^0 \overrightarrow{\varepsilon_1} e^{i(\omega_2 t - \overrightarrow{k_2}\cdot\overrightarrow{r} + \varphi_2)} \tag{7}$$

where ω_1, ω_2 are the respective angular frequencies, $\overrightarrow{k_1}, \overrightarrow{k_2}$ are the respective wave vectors, φ_1, φ_2 are the respective phases and $\overrightarrow{\varepsilon_1}, \overrightarrow{\varepsilon_2}$ are the respective polarizations.

When $\overrightarrow{E_1}$ and $\overrightarrow{E_2}$ are sent to a photodiode through the same optical fiber, the photodiode receives the sum $\overrightarrow{E_3} = \overrightarrow{E_1} + \overrightarrow{E_2}$ of the two signals. The intensity of the resulting signal $\overrightarrow{E_3}$ is of the following form

$$I = \left|\overrightarrow{E_3}\right|^2 = \left(\overrightarrow{E_1} + \overrightarrow{E_2}\right)\left(\overrightarrow{E_1}^* + \overrightarrow{E_2}^*\right) \tag{8}$$
$$= \overrightarrow{E_1}\overrightarrow{E_1}^* + \overrightarrow{E_2}\overrightarrow{E_2}^* + 2\,\Re\left(E_1^0 E_2^{0*} \overrightarrow{\varepsilon_1}\overrightarrow{\varepsilon_2}^* e^{i\left((\omega_1-\omega_2)t - \left(\overrightarrow{k_1}-\overrightarrow{k_2}\right)\cdot\overrightarrow{r} + \varphi_1 - \varphi_2\right)}\right), \tag{9}$$

where $\overrightarrow{\cdot}^*$ denotes the complex conjugate of $\overrightarrow{\cdot}$.

The beat signal produced by the photodiode is thus expressed as

$$s_{beat}(\overrightarrow{r}, t) = U \cdot \cos\left((\omega_1 - \omega_2)t - \left(\overrightarrow{k_1} - \overrightarrow{k_2}\right)\cdot\overrightarrow{r} + \varphi_1 - \varphi_2\right) \tag{10}$$

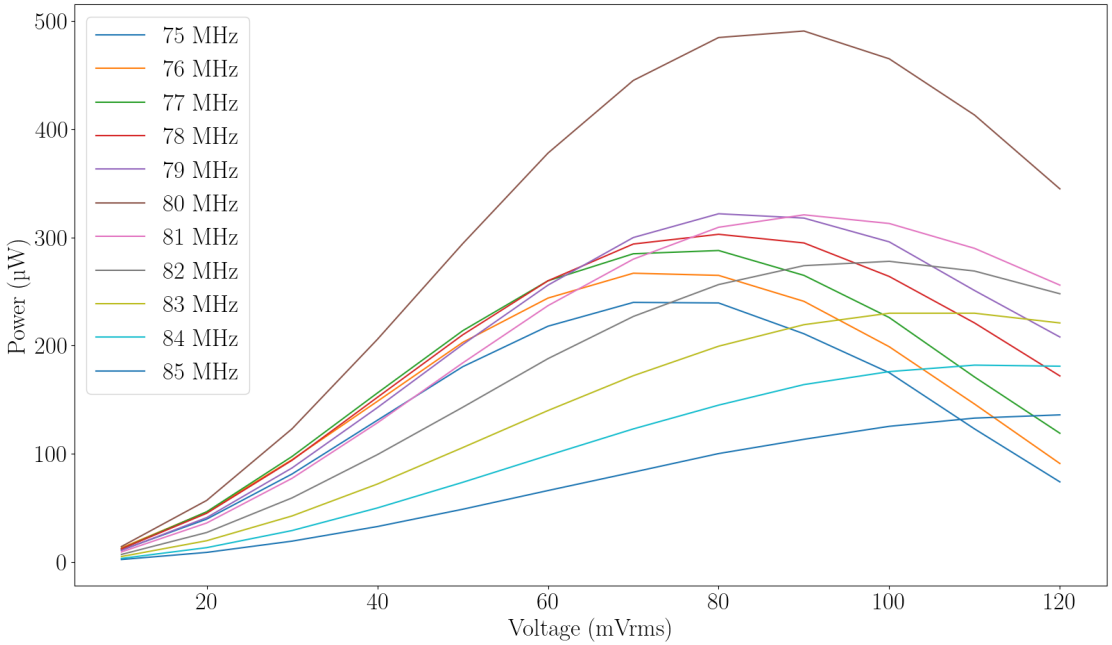

Figure 3: *Output power of the AOM depending on the voltage amplitude of the AOM-powering signal*

2.3 Theoritical tools

2.3.1 Decibel-milliwatts (dBm)

In radio-frequency engineering, AC power is expressed in dBm. This unit of power level is expressed relatively to a reference power $P_0 = 1$ mW. The relationships between power level x (expressed in dBm) and power P (expressed in mW) are

$$x = 10 \log_{10} \left(\frac{P}{1 \text{ mW}} \right) \qquad \text{and} \qquad P = 1 \text{ mW} \cdot 10^{\frac{x}{10}}. \tag{11}$$

One will keep in mind remarquable values : 1 mW = 0 dBm and 2 mW = 3 dBm.

2.3.2 Power spectral density

For a random variable $g(t)$ defined for all t, the power spectral density is the power distribution across the frequencies $(2\pi f_i)_i$ composing the signal.

Thanks to Wiener-Kintchine's theorem, it is known that the spectral density of $g(t)$ is equal to the squared module of its Fourier transform $G(\omega)$.

$$S_g(\omega) = |G(\omega)|^2 \tag{12}$$

3 Protocol

3.1 Current protocol

The optical signal whose noise needs to be cancelled is $A(t) = E_0 \cos(\omega_L t + \varphi)$ and is sent through a Michelson interferometer. As showed in figure 4.

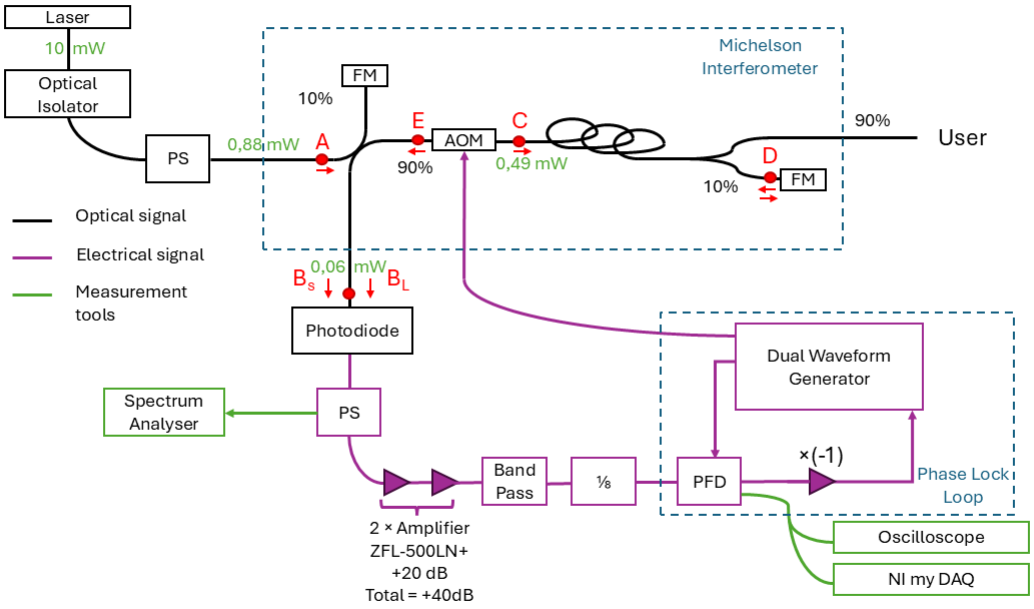

Figure 4: *Schematic diagram of the current phase-noise compensation system using a phase-frequency detector. The dual waveform generator is a Siglent SDG 6022X.*

In the "short arm", the signal is rapidly reflected on a Faraday mirror. The one-way phase induced by the short arm fiber is noted ϕ_{F_S} and that of the joint section between the arms is noted ϕ_{F_c}. Hence, the signal coming back from the short arm into the beam splitter is expressed as

$$B_S(t) = rtE_0 \cdot \cos\left(\omega_L t + 2\phi_{F_S} + \phi_{F_c} + \varphi\right), \tag{13}$$

where $r = \sqrt{R} = \sqrt{0.1}$ is the reflexion coefficient, and $t = \sqrt{T} = \sqrt{0.9}$ is the transmission coefficient.

In the "long arm", the signal is sent off to an acousto-optic modulator (AOM) which induces a frequency shift of Ω and a phase shift of ϕ_G, as recalled in (5) of section 2.1.3. At this point, the signal can be expressed as $C(t) = t \cdot \cos\left((\omega_L + \Omega)t + \phi_G + \varphi\right)$.

It passes through a long optical fiber, which induces a one-way phase noted ϕ_{F_L}. This is the phase noise that needs to be compensated. When the signal reaches the "client", a 90/10 power splitter is used to reflect back 1% of the power, using a Faraday mirror, thus leaving 90% of the power for the end user.

$$D(t) = rt \cdot \cos\left((\omega_L + \Omega)t + \phi_G + \phi_{F_L} + \varphi\right). \tag{14}$$

The signal that comes back from the long arm is also submitted to the same frequency and phase shift : $E(t) = rt^2 \cdot \cos\left((\omega_L + 2\Omega)t + 2\phi_G + 2\phi_{F_L} + \varphi\right)$. The optical signal that comes back from the long arm is thus expressed as

$$B_L(t) = r^2t^2E_0 \cdot \cos\left((\omega_L + 2\Omega)t + 2\phi_G + 2\phi_{F_L} + \phi_{F_c} + \varphi\right). \tag{15}$$

A photodiode then detects the beat signal of the two arms, and converts it to an electrical signal, as described in (10) of section 2.2.

$$s_{beat}(t) = S_b \cos\left(2\Omega t + 2\phi_C + 2\phi_F\right). \tag{16}$$

Note that it is essential for the two generators to be totally synchronized to avoid a phase drift that would prevent a phase correction.

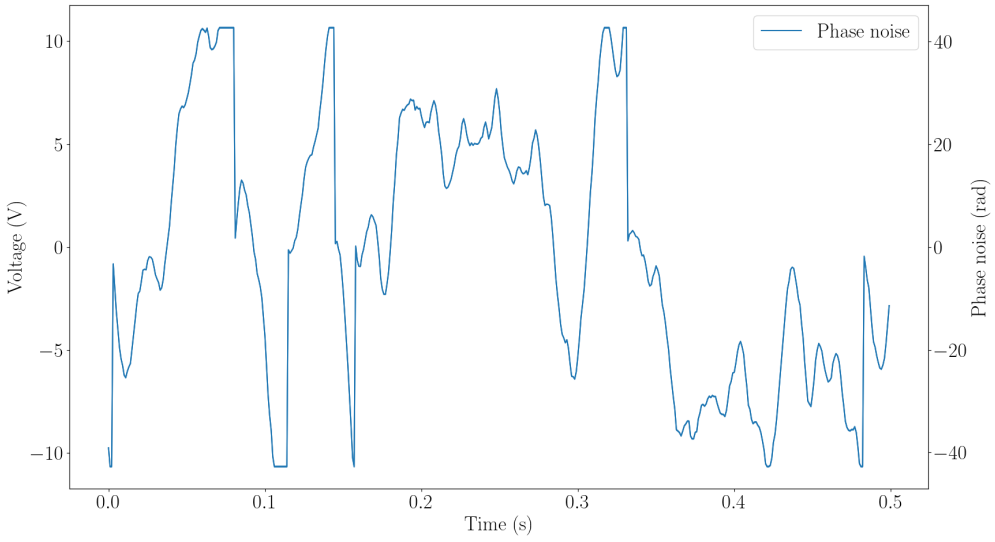

Figure 5: *Phase noise in 204.5 m of optical fiber(uncertainty : 30 mV)*

4 Results and discussion

4.1 Phase noise measurement and locking

The first result of our experiment is that our system effectively measures phase noise. To do so, we linked the output of the phase-frequency detector (PFD) to the oscilloscope and watched the signal obtained.

On Figure 5, a fast gitter of the phase noise can be seen. Owing to the $\frac{1}{8}$ divider in the PFD, the span of phase noise is 32π ($\pm 8 \times 2\pi$ for a lead or a lag which sums up to 32). The correspondance between voltage and phase is therefore 32π for the total 25 V voltage span available which gives $4.02\ \mathrm{rad} \cdot \mathrm{V}^{-1}$. Each time the phase noise goes beyond a $\pm 16\pi$ phase deviation, the measure jumps back to 0 instantly, explaining the measurements jump observed. The saturation observed is due to the acquisition tool used (NI myDAQ) whose voltage saturation is ± 10 V.

Second main result : the system perfectly locks the phase noise (with only 0.16 rad of phase variation remaining). The bandwidth of the spectrum seen in Figure 6 is thus thinner. Figure 6 also shows the influence of the frequency deviation (which is akin to the gain of our PLL), on the beat spectrum. A frequency deviation has been found optimal 300 kHz as it thins the central peak without heightening too much the side wings.

4.2 Characterisation of the phase noise in the building

4.2.1 Correction frequency for phase measurement and short term results

Thanks to the lock, we can measure the phase noise by indirectly measuring the frequency deviation produced by the FM modulation in the PLL. It is indeed linked to the phase noise through the following equation :

$$f(t) = \frac{1}{2\pi} \frac{\mathrm{d}\phi}{\mathrm{d}t}. \tag{17}$$

The counter used to measure the frequency is a Keysight 53230A. What it actually measures is the phase increment between two samplings giving the following equation.

$$f(t) = \frac{\phi(t) - \phi(t-\tau)}{2\pi \times \tau}, \tag{18}$$

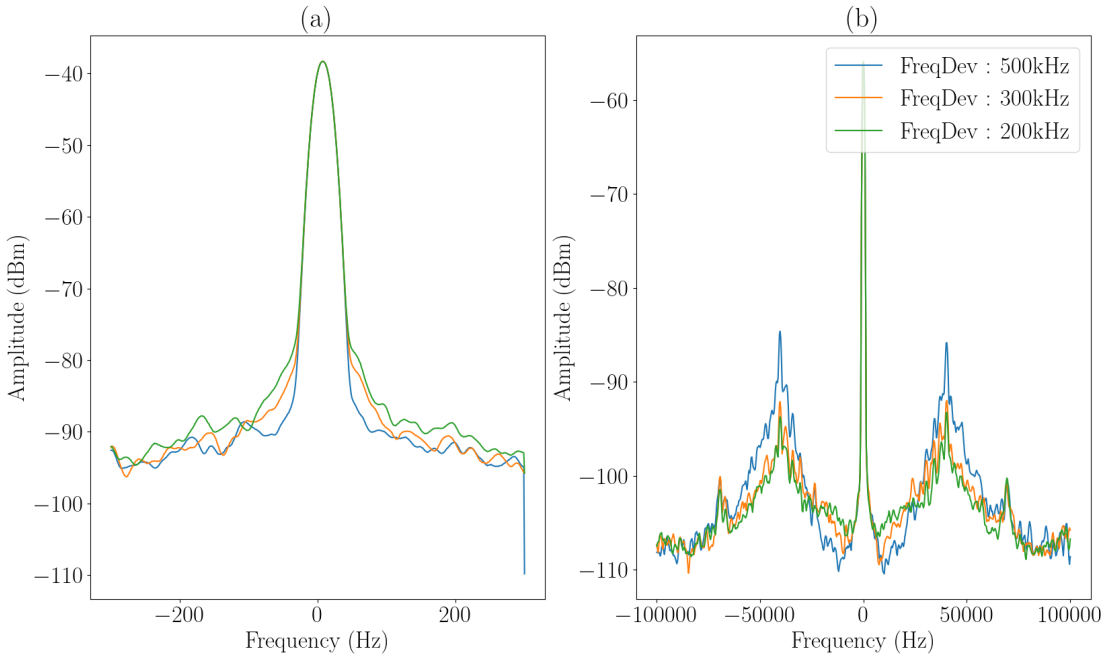

Figure 6: *Beat spectrum for a 204.5 m configuration with Phase lock loop turned on (a) Span of* 1 kHz *(b) Span of* 200 kHz *Center frequency :* 160 MHz

where τ is the sampling time, and f the correction frequency which corresponds to the phase noise. From this equation 18, we deduce equation 19 to reconstruct the phase signal :

$$\phi_N = \sum_{k=0}^{N} 2\pi\tau f_k, \tag{19}$$

where τ is the sampling time, $f_k = f(k\tau)$ and ϕ_N is the phase on time $N\tau$.

The results obtained through this method for a 615.5 m optical fiber configuration are displayed on Figure 7. Figure 8 shows that the noise mainly comes from low frequency phenomenon which could be of thermal origin. To further study the noise we did a long term measure over two weeks during the winter holidays of 2024.

4.2.2 Long term evaluation and link between phase noise and temperature

As seen in Figure 9, the phase noise during the 2024 end of year holiday has a span of about 100000 rad.

The origin of the phase noise is the variation in optical path which can have many different origins. One of the main sources is the variation of outer temperature. Indeed, the variation of temperature can induce a dilatation of the silicium composing the fiber, thus increasing or decreasing the length of said fiber. A change in temperature also causes a change in the optical index.

Mathematically, these phenomenon translate as such. First, the optical path is defined by :

$$\widehat{L} = n_{eff} L, \tag{20}$$

where n_{eff} is the effective refraction index in SiO_2 single mode fiber and L is the total length of the optical fiber.

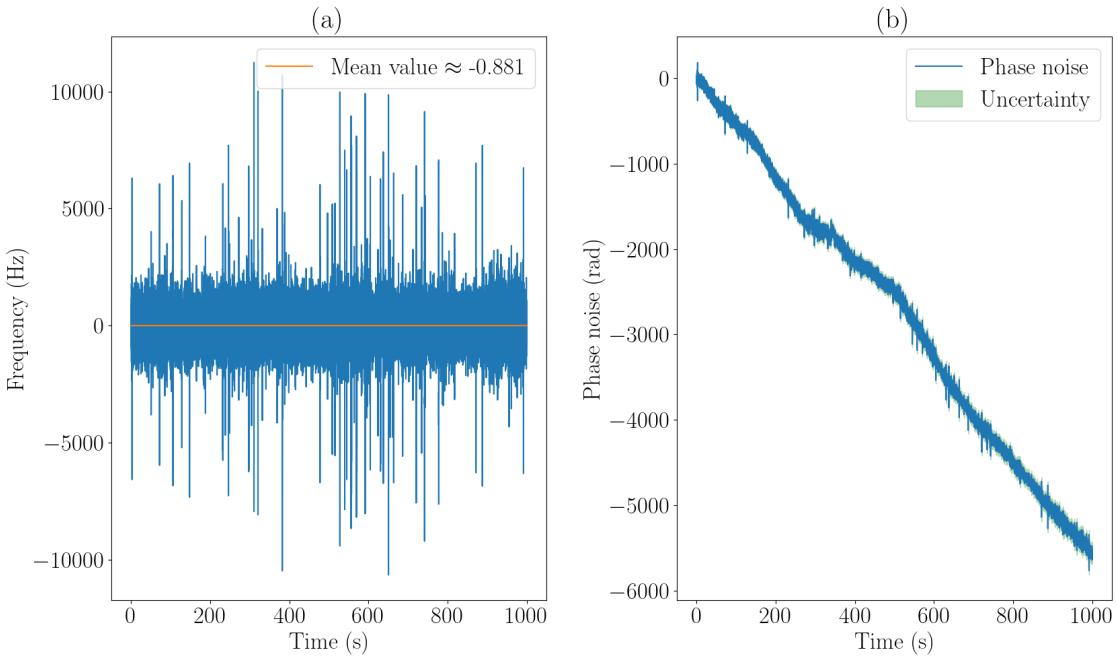

Figure 7: *Measures using the correction frequency for 615.5 m of optical fiber (a) Frequency correction (Uncertainty : 8 Hz) (b) Phase noise calculated with Eq 19*

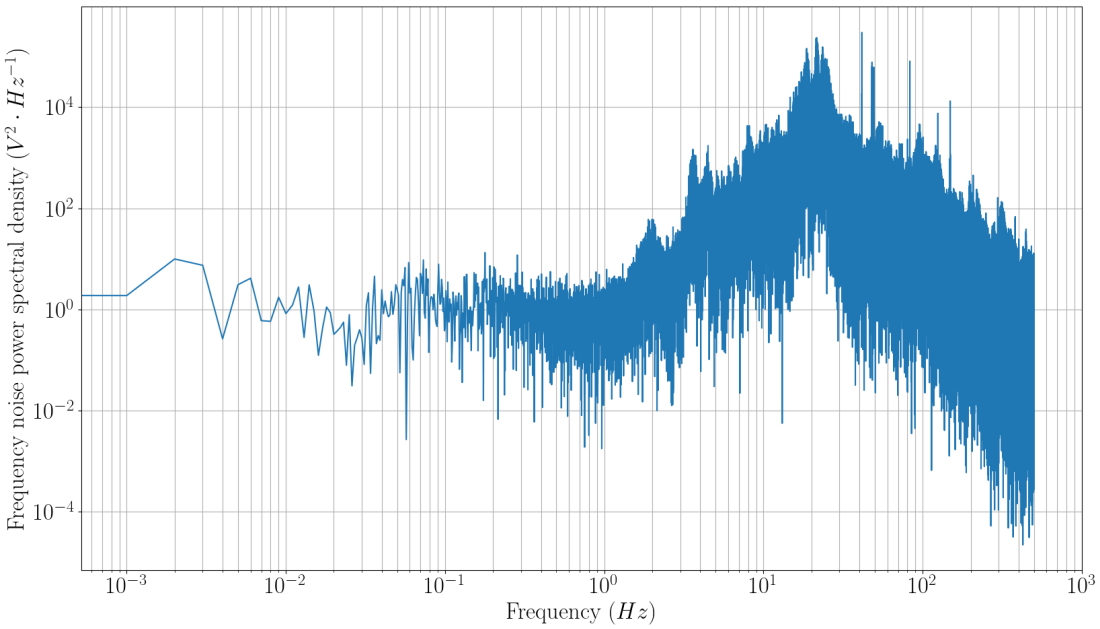

Figure 8: *Frequency noise power spectral density*

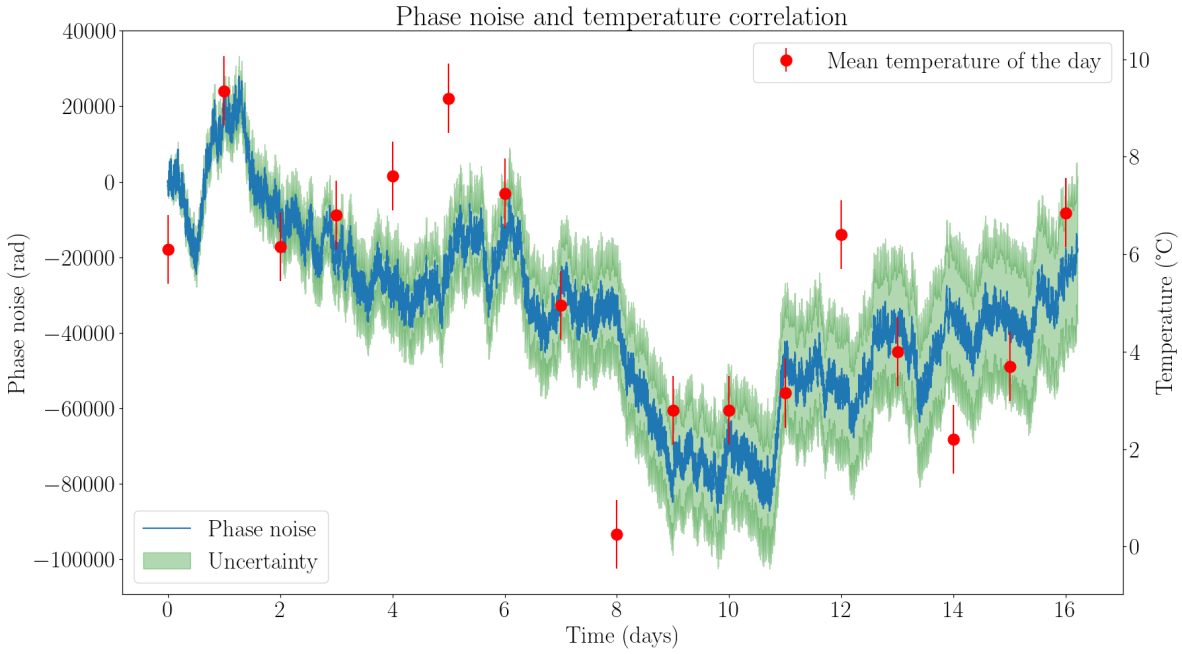

Figure 9: *Correlation between outer temperature and phase noise between 20/12/2024 and 05/01/2025 Uncertainty of temperature measure: 1°C*

The total variation of the optical path due to temperature effect is therefore :

$$\frac{\mathrm{d}\widehat{L}}{\mathrm{d}T} = \frac{\partial L}{\partial T} n_{eff} + \frac{\partial n_{eff}}{\partial T} L = L\left(\frac{1}{L}\frac{\partial L}{\partial T} n_{eff} + \frac{\partial n_{eff}}{\partial T}\right), \tag{21}$$

which gives two contributions, the second one being dominant.

For the silica used in monomode fibers, the factors are reported to be : $\frac{1}{L}\frac{\partial L}{\partial T} = 5.10^{-7}\ °\mathrm{C}^{-1}$ and $\frac{\partial n_{eff}}{\partial T} = 8,5.10^{-6}\ °\mathrm{C}^{-1}$ [**?**].

The measures realised were done with an optical fiber of 204.5 m and the distance traveled by the light is 410 m, Eq 21 therefore gives $\frac{\Delta\widehat{L}}{\Delta T} = 3,78.10^{-3}\ \mathrm{m}\cdot°\mathrm{C}^{-1}$, multiplying by $\frac{2\pi}{\lambda}$, we get 15000 $\mathrm{rad}\cdot°\mathrm{C}^{-1}$ at 100000 rad. When compared with the 1542 nm span of phase noise, if we assume that the majority of the long term phase noise is caused by the variation of temperature, the value corresponds to a variation of about 6 to 7 °C which is possible due to building heating reduction during the holidays. To corroborate this hypothesis, we compared the long scale variation of the phase noise during the span of two weeks with the variation of temperature during the same period.

On Figure 9, even if the correlation is not absolute, the variation of temperature and the variation of the phase noise follow the same long term trend. It is reasonable to assume that temperature is the leading contribution to long term phase noise.

N.B. : To display the uncertainty in Figure 9, we used Equation 19 coupled with the following hypothesis. With an uncertainty of about $\sigma_f = 8$ HZ in the frequency measurement, and if we assume that each measurement is independant of the preceding one and following a gaussian distribution, the formula obtained for the uncertainty of the phase at time N is :

$$\sigma_{\phi_N} = 2\pi\sigma_f\sqrt{N}. \tag{22}$$

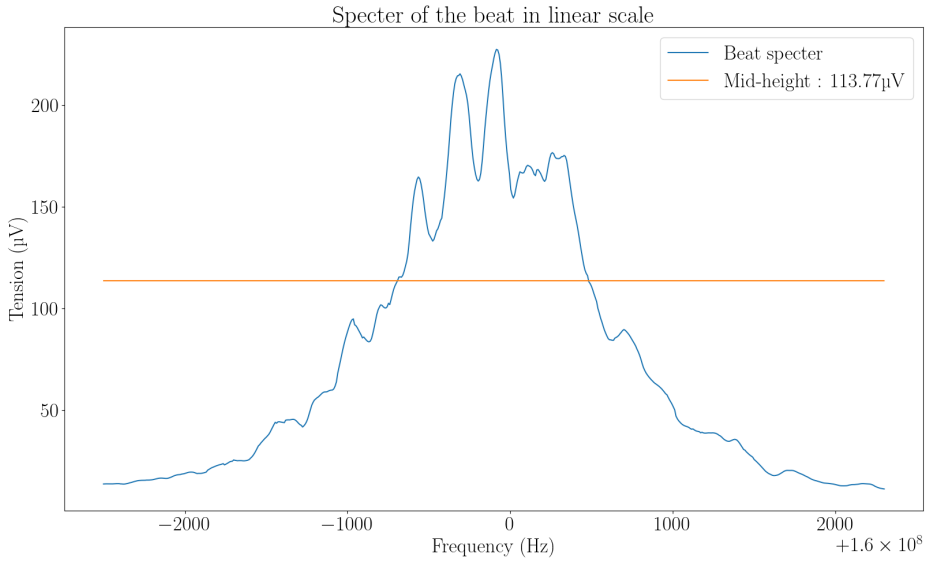

Figure 10: *Specter of the beat in the configuration with a* 615.5 m *optical fiber*

The same logic was used to display the uncertainty of Figure 7.

4.2.3 Effect on the Full Width at Half Maximum (FWHM)

To determine the real impact of the phase noise on the experiment done by the LKB-Trapped Ions team, the broadening of the bandwidth of the laser comb had to be estimated. The measures of the FWHM were done through two different methods.

Direct method using a spectrum analyser
In the first method the beat signal is displayed on a spectral analyserand the FWHM is easily determined as seen on Figure 10. The results of the FWHM for various optical fiber lengths have been recorded in Table 1.

β-intersection line method
The other method uses the Beta line intersection method which we studied based on the articles *Extra-cavity laser band-shape and bandwdth modification* [**?**] and *Simple approach to the relation between laser frequency noise and laser line shape* [**?**].

The resulting formula is as follows :

$$FWHM = \left(8\ln(2) \times \int_{1/T_0}^{\infty} H\left(S_{\delta\nu}(f) - \frac{8\ln(2)f}{\pi^2} \right) S_{\delta\nu}(f) df \right)^{\frac{1}{2}}, \tag{23}$$

where $S_{\delta\nu}(f)$ is the frequency noise power spectral density, $H(x)$ is the Heaviside unit step function ($H(x) = 0$ if $x < 0$ and 1 otherwise) and T_0 is the measurement time preventing observation of frequencies lower than $1/T_0$.

In concrete terms, to access the FWHM, the frequency noise density spectrum is to be plotted alongside the Beta intersection line whose equation is $y = \frac{8\ln(2)}{\pi^2} f$, and then only the part of the density that is "on top" of the line is to be integrated to access the FWHM. The principle is shown in Figure 11.

The results of both methods have been recorded in the following Table

The results of Table have been displayed on Figure 12 based on the direct measures. We have observed that the FWHM seems to increase proportionnaly to $\sqrt{L}$ with L being the length of the fiber. We have displayed the resulting line based on Table 1 on Figure 12.

03/10/2025 LH : Les longueurs effectives de propagation sont en fait deux fois plus longues qu'indiqué, soit 0, 20, 41, ... 1231 m. La pente de la courbe de la figure 12 est donc 1530 Hz^2/m, d'où un élargissement de 39 Hz/racine(m)

Optical Fiber length (m)	0	10	20.5	102	204.5	615.5
Spectral Analyser measured FWHM (Hz)	0	190 ± 2	128 ± 3	442 ± 20	866 ± 50	1359 ± 50
Beta-Intersection-line measured FWHM (Hz)	xx	41	44	174	327	1023

Table 1: FWHM of the phase noise measures

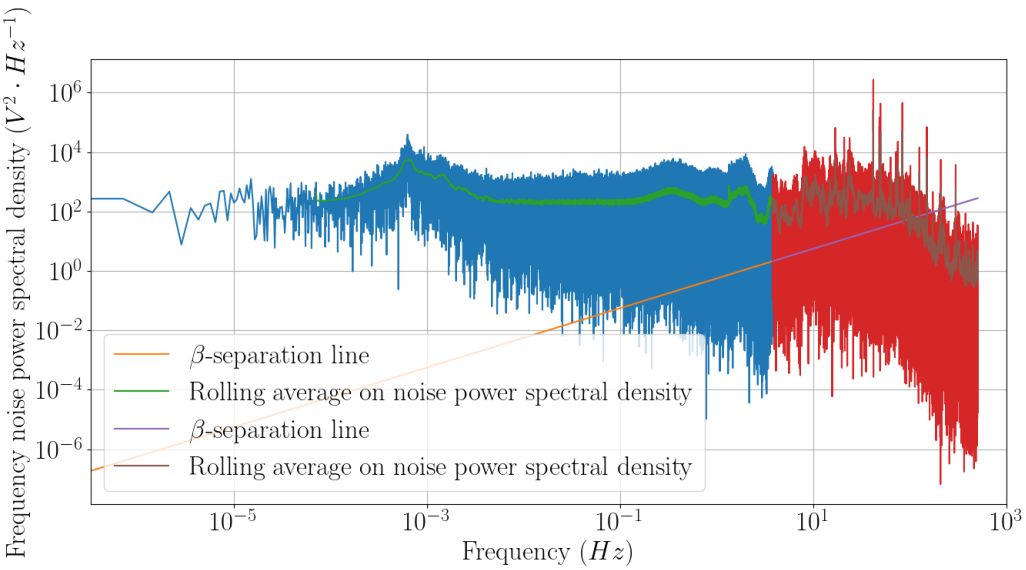

Figure 11: *Frequency noise power spectral density of a* 204.5 m *optical fiber. The high frequencies and low frequencies have joined together*

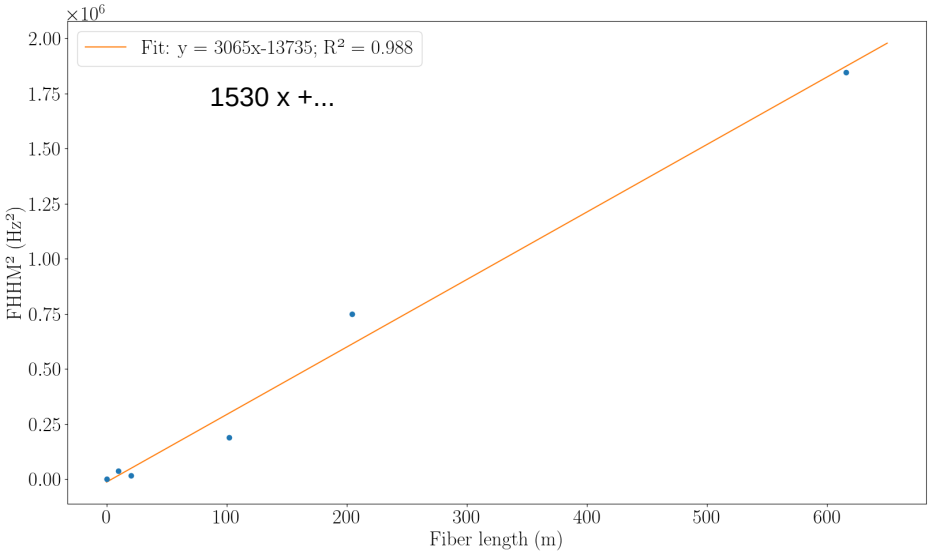

Figure 12: *FWHM² depending on the length of optical fiber*

To explain this relationship, we can assume that the noise added on a section s of the fiber is independant from the noise generated by the section s'. If we also assume that the noise is gaussian, than we

Component	Voltage (V)
Photodiode (Hz)	15
Phase frequency detector (PFD)	±15
2× ZFL-500LN+ Amplifiers	15
Inverting amplifier	±15
AOM	12

Table 2: Voltage needs for various components

State	Current for the outlet	
	+15 V (mA)	-15 V (mA)
Phase locked	371	22
Unlocked	373	25

Table 3: Current needs for ±15 V outlets

can deduce that the variance of the fiber noise is :

$$\Delta\nu_{RMS}^2 = \int_0^L Variance(s)ds = KL, \tag{24}$$

with L being the length of the fiber and K a proportionality coefficient.

According to Eliott's article [**?**], the FWHM of phase noise is given by :

$$FWHM = K'\Delta\nu_{RMS} = \eta\sqrt{L}, \tag{25}$$

where η is the proportionality coefficient.

According to Figure 12, we deduced a coefficient of 55 Hz/$\sqrt{\text{m}}$ which is the third main result of our experiment.

39 Hz/racine(m)

5 Set up of the system

Afted having experimented on a first prototype and compiled the preceding results, we had to compact the system for its actual use by the LKB Trapped Ions Team. We designed a storage rack for our system which is to be put in the REFIMEVE extration station. In order for it to be adapted to the shelve in the extraction station, we bought a 19 inch wide rack (standard width) which is wide enough to store three compensation systems next to each other. When designing this rack, a few challenges arose.

5.1 Electrical powering

In the end, our system used many electrical components that had to be powered simultanously. The differents components and their needs have been summed up in Table 2

We also measured the global current need for the ±15 V power output :

To ensure that three whole systems could be powered, we bought a TRACO Power TXL 035-1515D that has enuogh power outlets and output currents of 2.4 A and 1.5 A.

5.2 Design

As seen on Figure 13, we designed a two story storage with the electrical components on top of a elevated table and the fibers put underneath it on a plastic cussion to avoid vibrations.

6 Conclusion

6.1 Phase noise compensation and next steps

The conclusion of this paper is that a compensation of the phase noise is indeed needed for the applications in LKB, with 55 Hz/$\sqrt{\text{m}}$ being a significative deterioration of the signal. The phase lock system works and will be set up to effectively help stabilize the signal in LKB. The next step would be to put the system in the REFIMEVE extraction station and to link it to a router in order for it to be remotely controled in the lab room.

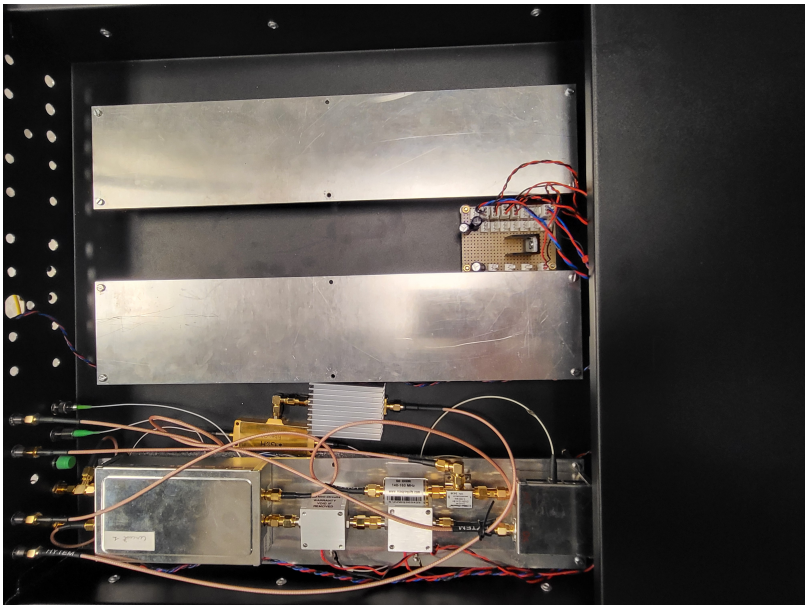

Figure 13: *System inside the rack*

6.2 Future improvements

The system that we set up still has some flaws that could be adressed.

First is that we could shorten the length of the fiber used in the compensation system itself, which still sum up to about 2 m, thus deteriorating the signal. The second major improvement of the implemented system would be a better management of the heat in the system which was totaly overlooked. For example, we used a 15 V powering system to power the PFD when it only needs 5 V to work, thus creating lots of heat.

Thanks

We would like to thank our tutor; Laurent Hilico, for his heartwarming support throughout this internship.